The Physical Metallurgy of Nitinol for Medical Applications

Alan R. Pelton, Scott M. Russell, and John DiCello

Journal of Metals, 33-37, May 2003.

2003

The Physical Metallurgy of Nitinol for Medical Applications

Alan R. Pelton, Scott M. Russell, and John DiCello

The purpose of this paper is to review the current processing and resultant properties of Nitinol for medical device applications. The melting and fabrication of Nitinol present a number of unique challenges because of the strong sensitivity of the alloy system to chemistry and processing. The first part of this paper will summarize the effect of alloy fabrication on key material properties, vacuum-melting techniques, hot working, and cold working. The effects of the final shape-setting heat treatments on transformation temperature and mechanical properties for medical devices will also be reviewed.

INTRODUCTION

The growth of the use of Nitinol in the medical industries has exploded in the past ten years due to increasing demand for minimally invasive surgical and diagnostic procedures. Nitinol is the enabling component in an increasing number of devices such as endoscopic instruments, stents (see Figure 1), filters, and orthopedic devices; examples of these medical applications are richly illustrated in other publications.[1–5] The preference for Nitinol over more standard engineering alloys is based on its unique combination of mechanical properties, including shape memory and superelasticity, coupled with superb biocompatibility.[5]

The physics of the phase transformations that give rise to the shape-memory effect in Nitinol have been known since the 1960s and have been the source of many technical articles and books.[6–11] However, Nitinol producers have only recently focused on optimizing processes for a few standard alloys rather than pursuing a myriad of "boutique alloys" with niche applications. The industry workhorse alloy is 50.8 at% nickel–49.2 at.% titanium, hereafter referred to as $Ni_{50.8}Ti_{49.2}$. This alloy is used in many thousands of kilometers of wire and microtubing for such diverse products as cellular telephone antennas, eyeglass frame components, guidewires, undergarment supports, and orthodontic archwires.

To ensure the quality and consistency of the Nitinol materials used in medical devices, it is important to understand some of the fabrication processes and their effects on the final properties and performance. Therefore, the purpose of this paper is to summarize Nitinol processing methods from the selection of raw components and melting practices to hot working and cold working. Additionally, the metallurgical influences of time and temperature for shape setting will be illustrated with examples.

NITINOL PHASE TRANSFORMATIONS

The unique shape-memory and superelastic properties of Nitinol are due to a diffusionless phase transformation between a higher-temperature austenite phase (B2 structure) and a lower-temperature martensite phase (B19´ structure).[6–11] The hysteresis curves that characterize the thermal and mechanical behavior are explained in great detail in these publications. For many medical devices, the temperature at which martensite fully transforms to austenite (A_f) is the most important transformation temperature since it dictates the transition between shape memory and superelastic properties. As will be discussed in this article, the A_f temperature can be adjusted through thermomechanical treatments in order to optimize device performance.

Nitinol can be considered an ordered intermetallic that has an extremely narrow composition range below the 630°C eutectoid as shown in the binary phase diagram (refer, for example, to Reference 11). Therefore, any deviation from the stoichiometric 50:50 composition requires that the alloy is in a two-phase field. Slight deviations in composition also affect the transformation temperatures, which are determined by the nickel and titanium ratio. As

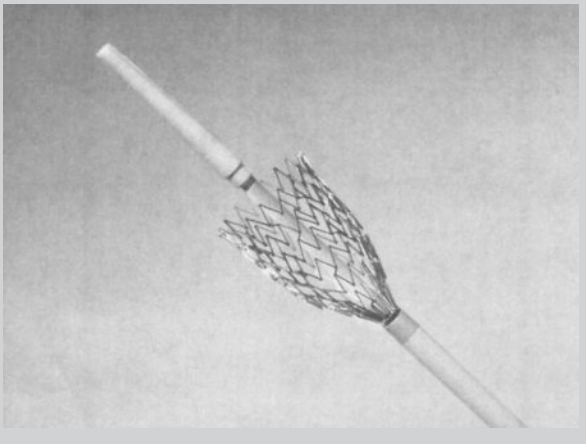

Figure1. A Cordis Corporation SMART Nitinol endovascular stent that was manufactured through processes outlined in this paper.

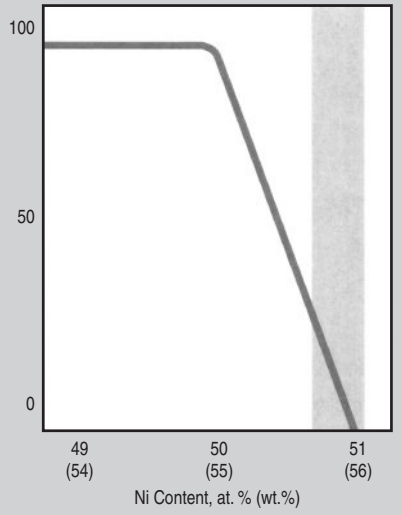

Figure 2. A schematic of the effect of the nickel content in Nitinol on the alloy phase transformation temperature, A_f. Note that a very small change in alloy composition can have a very large effect on the transformation temperature. The shaded region represents the area covered by typical binary superelastic Nitinol alloys.

shown in Figure 2, a 1% shift in the amount of either nickel or titanium in the alloy will result in a 100°C change in alloy-transformation temperature. Most applications require the alloy-transformation temperatures to be controlled within ±5°C, which means that the alloy composition must be controlled within ± 0.05%. These compositional requirements are significantly tighter than 300 series stainless steel. Furthermore, most standard chemical-analysis methods are not precise enough to measure such subtle differences in alloy composition, so a differential scanning calorimetric measurement of the alloy-transformation temperatures is used to confirm proper ingot formulation.[12]

The presence of impurities in Nitinol can affect the transformation temperatures of the material as well as the mechanical properties (see Table I). Most impurities depress the transformation ("down" arrows); they react with the titanium in the melt to form precipitates, resulting in nickel enrichment in the base alloy. As illustrated in Figure 2, higher nickel contents tend to lower the transformation temperature. For example, titanium strongly reacts with oxygen, nitrogen, and carbon to form oxides, oxi-nitrides, and carbides; therefore, the melting methods are selected to minimize their presence. Copper and niobium do not directly decrease the transformation temperature, although copper additions modify the phase transformation, and niobium has virtually no solubility in the NiTi phase.[13] Chromium, cobalt, and iron all substitute for nickel in the B2 lattice and, therefore, have an additive effect in determining the transformation temperature. In turn, most of these impurities simultaneously increase the strength of the ingot and decrease the ductility. Recent ASTM specifications set strict limits on these impurities for medical-grade binary Nitinol.[14]

Table I. A Schematic Table Illustrating the Effects of Various Melting Impurities on the Resulting Ingot Properties*

	O	N	H	C	Cu	Cr	Co	Fe	V	Nb
Temperature	↓	↓	↓	↓	→	↓	↓	↓	↓	→
Strength	↑	↑	↑	↑	↘	↑	↑	↑	↑	↑
Ductility	↓	↓	↓	↓	→	↓	↓	↑	↓	→

* See text for explanation of the symbols.

MELTING METHODS

The sensitivity of the transformation temperatures to alloy composition is an important consideration in selecting an alloy melting method. As discussed previously, any contaminant will affect the amount and chemistry of phases present, possibly resulting in an unusable material. Therefore, both an alloy melting method and the elemental raw materials must be chosen to ensure high purity. Further, the melting method must be one in which the molten material is very well mixed throughout to achieve ingot homogeneity and uniformity of properties. As such, the two most common commercial melting methods are vacuum-induction melting (VIM) and vacuum-arc remelting (VAR).[15,16] Both melting methods start with high-purity components of nickel (>99.94% purity) and titanium (>99.99% purity).

For VIM ingots, the nickel and titanium are weighed out in the proper ratio and placed in an electrically conductive crucible (usually graphite) inside a vacuum chamber, as shown schematically in Figure 3. The crucible is heated from the outside by electrical induction coils. Once the constituents are molten, the induction fields stir the alloy completely, which results in a homogeneous melt. Homogeneity is confirmed in the solid ingots, where transformation temperature uniformity within a degree or two is achievable. The main disadvantage of VIM is that the molten Nitinol picks up a small amount of carbon contaminant from the graphite crucible. Carbon impurity levels of 300 wppm to 700 wppm are typical for VIM-melted materials. Major commercial suppliers of VIM Nitinol

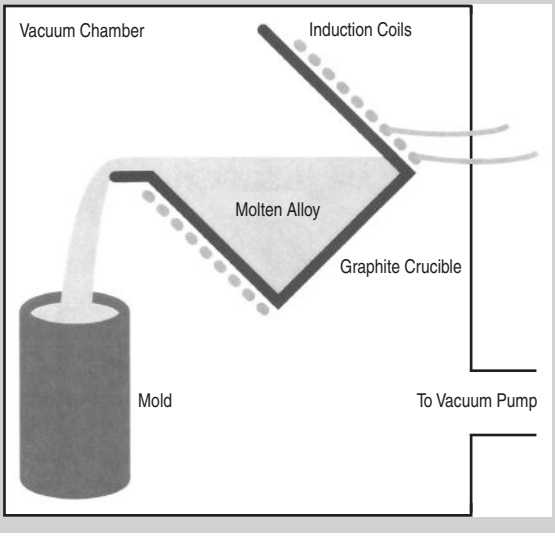

Figure 3. A schematic of vacuum-induction melting.

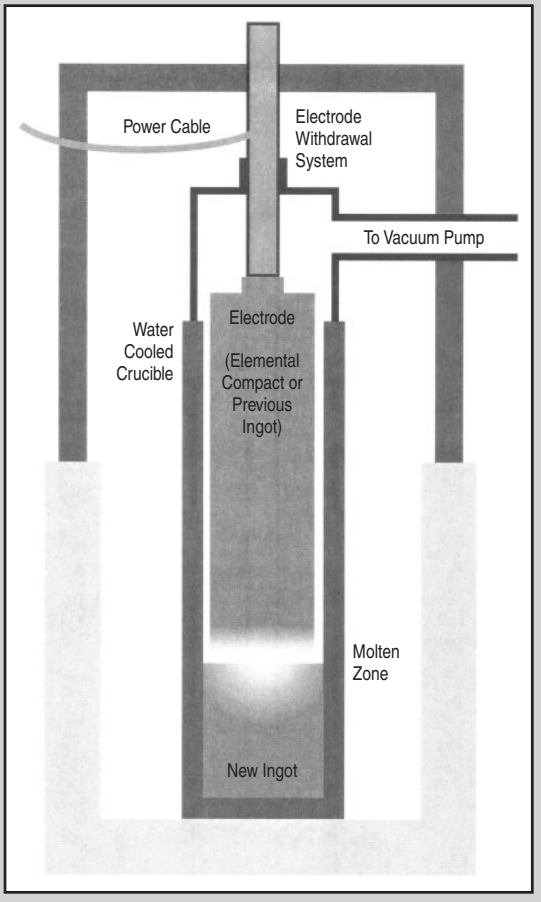

Figure 4. A schematic of vacuum-arc remelting.

include Furukawa Electric (Japan) and Special Metals (United States).

In VAR melting, the nickel and titanium are weighed out in the proper ratio and are pressed into a large compact, which is used as a consumable electrode. An electrical arc is initially struck between the electrode and the bottom of the crucible and sufficient current is passed to melt the electrode continuously (see Figure 4). As molten metal is formed, the electrode is slowly withdrawn and the metal solidifies at the bottom of the melt pool. The molten pool is contained by a water-cooled copper crucible that forms a frozen skull on the outside of the pool, preventing any contamination of the melt by the crucible. Because of this, VAR melting achieves extremely high purity of the resultant alloy. The disadvantage of this method is that the entire ingot is not molten at the same time; consequently, the ingot is remelted several times to achieve high homogeneity. Vacuum-arc remelting is also used for further refining of VIM ingots; the final products are known as VIM/VAR ingots. The major commercial supplier of VAR Nitinol is Wah Chang (United States).

References 15 and 16 summarize the differences between VIM and VAR melting. In general, the cost of Nitinol produced by either technique is similar. Further, the major commercial suppliers of Nitinol around the world are currently producing acceptable high-quality materials for the exacting needs of the medical device industry by either melting method.

HOT WORKING

Commercial VAR or VIM/VAR ingots are generally 50 cm in diameter and weigh in excess of 2,500 kg. Hot-working processes are typically used to reduce the cross-sectional dimension to less than 15 cm. Depending on the final product shape, techniques such as press forging, rotary forging, extrusion, swaging, bar rolling, rod rolling, and sheet rolling may be used in the hot-working stage. Hot working is typically performed at temperatures of 600°C to 900°C. These elevated temperatures (approximately 0.55–0.75 T_m) are sufficient to lower the flow stresses to allow relatively large deformation steps. In addition to dimensional reduction, these initial hot-deformation processes are effective in breaking up the as-cast microstructure, which has very little ductility and does not exhibit much shape memory, superelasticity, or resistance to fracture.

COLD WORKING

Cold-working processes provide the final product shape, surface finish, refined microstructure, and mechanical properties. Figure 5 shows the change in the ultimate tensile strength of cold-drawn 1 mm diameter wire. As illustrated in this figure, Nitinol alloys work harden rapidly, so the material must be fully annealed (at 600°C to 800°C) after cold-working operations. A series of such cold-working and annealing steps are usually required to bring the material down to its finished size. Figure 6a and 6b shows the microstructures of as-drawn and fully annealed 1 mm diameter wires, respectively. The as-drawn microstructure consists of deformed martensite and a high density of dislocations. The annealed grain size is ASTM 4 or finer (on the order of 100 μm).

Typical cold-worked Nitinol (semi-finished) products include wire, tubing, and sheet. For most applications, however, Nitinol does not exhibit the final desired properties in its cold-

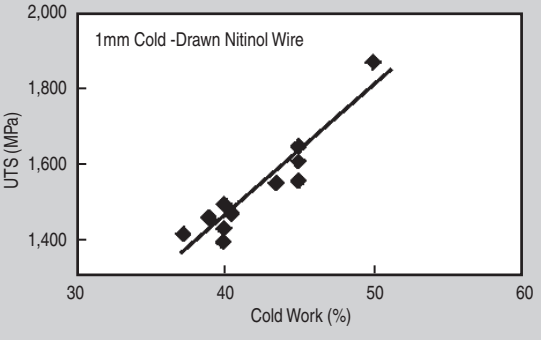

Figure 5. The effect of cold work on the ultimate tensile strength of a $Ni_{50.8}Ti_{49.2}$ Nitinol alloy. Note the high work-hardening rate.

a

0.1 μm

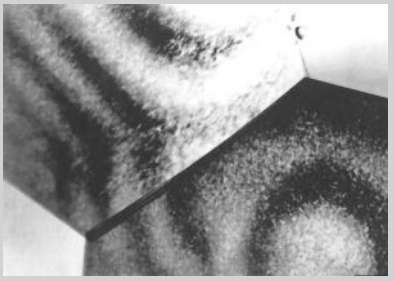

b

0.1 μm

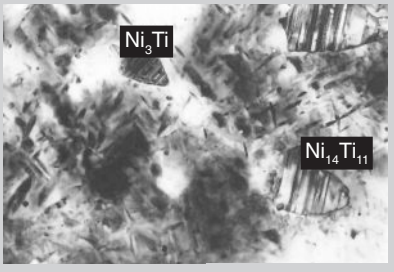

c

0.5 μm

Figure 6. The microstructures of (a) 40% cold drawn, (b) fully annealed, and (c) over-aged $Ni_{50.8}Ti_{49.2}$ alloys. The cold-worked structure consists of deformed martensite and a high density of dislocations. Annealed austenite forms well-developed equiaxed grain structures. The aged microstructure consists of $Ni_{14}Ti_{11}$ and Ni_3Ti precipitates.

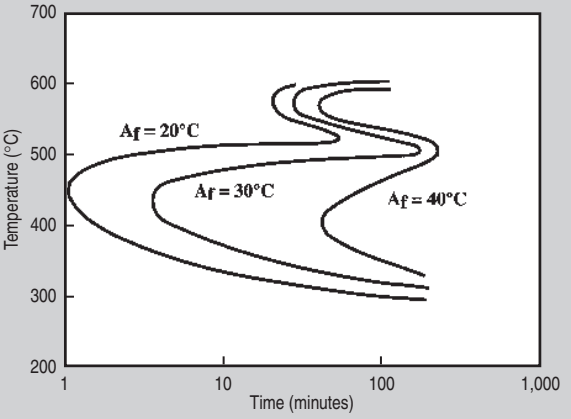

Figure 7. The effects of aging temperature and time on the transformation temperature of $Ni_{50.8}Ti_{49.2}$ wire with a starting A_f temperature of 11°C. The data are plotted to illustrate a novel A_f-TTT diagram. Note that the maximum precipitation rate is at about 450°C. Between 500°C and 600°C the precipitates re-solutionize and tend to lower the A_f. A new precipitate forms at longer times at these higher temperatures.

worked or fully annealed conditions. To optimize superelastic and shape-memory performance, the material must be partially heat treated after the final cold-working step.

SHAPE SETTING

In general, shape setting involves a combination of strain, temperature, and time to optimize the "remembered" shape. For example, the stent shown in Figure 1 was laser cut from Nitinol microtubing, shape set by expansion on a mandrel of a specific diameter, and then heat treated. Nitinol wires and tubes are continuously strain annealed to ensure that the entire length has uniform properties. Continuous strand straightening usually occurs in a temperature range of 450°C to 550°C under a stress of 35–100 MPa, depending on the requirements of the application. As the wire moves through the heat zone, it will initially try to shrink in length and grow in diameter due to the shape-memory effect not suppressed by the cold work (i.e., springback). As the wire reaches the furnace temperature, the internal stresses will begin to relax with a concomitant decrease in wire strength. Under these conditions, the applied stress induces strain, which shape sets the wire straight. Strains have been measured on the order of 2–3% during the wire-straightening process.[17,18]

The final heat treatment controls the final properties of the product, including shape, mechanical properties, and the active A_f. Longer times or higher temperatures tend to anneal the product, but result in more exact shapes with less springback. At the other extreme, shorter times or lower temperatures leave the material closer to the high-strength, cold-worked state with more shape springback. A balance must be developed between these two conditions to optimize the shape, A_f, and mechanical properties.

EFFECTS OF AGING TREATMENTS ON A_f

Several investigators have shown that optimal superelastic performance can be achieved in Nitinol alloys that have a combination of cold work and aging heat treatments.[17–20] Precise control of these thermomechanical treatments can lead to reproducible mechanical properties and transformation temperatures. Nickel-rich Nitinol alloys respond well to aging heat treatments to tune in the desired properties.

Nishida et al.[21] established the effects of aging time and temperature on the precipitation reactions in 52 at.% nickel–48 at.% titanium alloys by various metallographic techniques. They observed a precipitation sequence of $Ni_{14}Ti_{11} \rightarrow Ni_3Ti_2 \rightarrow Ni_3Ti$ at temperatures between 500°C and 800°C and for times up to 10,000 hours and presented their data in a time-temperature-transformation (TTT) diagram. A similar approach was demonstrated for the A_f changes of $Ni_{50.8}Ti_{49.2}$ wire that was cold drawn 42% and continuously straightened, as described previously. The wire had an initial A_f of 11°C, which is appropriate for many endovascular guidewire applications.[17,18] Figure 7 shows the A_f-TTT diagram, where each c-curve represents the loci of time and temperatures that produce a constant A_f after thermal treatments between 300°C and 600°C and for times up to 180 min. This figure demonstrates that there is a maximum in the precipitation reaction at about 450°C (i.e., the A_f increases most rapidly after heat treatments at 450°C). From an industrial standpoint, this indicates that slight variations in heat-treatment times at these temperatures may greatly affect the A_f. On the other hand, heat treatments around 300°C or 500°C tend to be less affected by time fluctuations.

The A_f changes shown in this figure

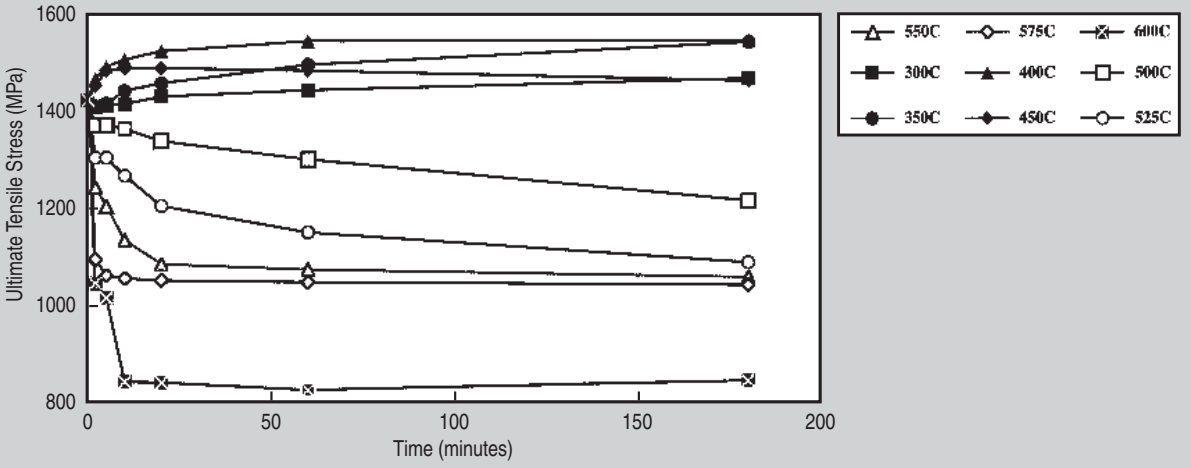

Figure 8. The effect of aging time and temperature on the ultimate tensile strength. Aging temperatures between 350°C and 450°C tend to increase the tensile strength due to precipitation hardening. Between 500°C and 600°C, annealing effects dominate with a dramatic decrease in the strength.

are due to precipitation reactions as discussed by Nishida et al.[21] As the volume fraction of these precipitates increases, the matrix becomes enriched in titanium and the A_f increases according to the relationship shown in Figure 2. These shifts of composition strongly affect the transformation temperatures even though the overall composition of the material remains unchanged. Figure 6c shows the microstructure of an overaged sample with a high volume fraction of nickel-rich precipitates.

These A_f-TTT diagrams can be used as tools to tune the transformation temperatures of the Nitinol products. For example, imagine that the stent discussed previously was heat treated at 400°C for 30 min. with a resultant transformation temperature of 37°C. If the specification calls for a maximum A_f of 30°C (just below body temperature), then the stent can be tuned to the proper A_f at 515°C for 2–3 min. The $Ni_{14}Ti_{11}$ precipitates that formed during the initial 400°C treatments will re-solutionize at 515°C, with a corresponding decrease in the transformation temperature as the nickel atoms diffuse back into the matrix. At longer aging times above 500°C, the Ni_3Ti_2 phase forms, with a corresponding increase in A_f.

EFFECTS OF AGING TREATMENTS ON ULTIMATE TENSILE STRENGTH

The wire used for the A_f-TTT diagram had an as-drawn ultimate tensile strength (UTS) of 1,550 MPa, which was reduced to 1,400 MPa during the straightening process. Figure 8 shows that the aging treatments also have an effect on the UTS. For example, aging between 300°C and 450°C increases the UTS, which demonstrates that the $Ni_{14}Ti_{11}$ precipitates are effective barriers to dislocation motion and act to strengthen the matrix. At higher temperatures (500–600°C), however, the UTS decreases even though precipitates form during aging. The decrease in UTS at these higher temperatures reflects that the onset of recrystallization begins around 475°C and that the Ni_3Ti_2 precipitates are less effective in strengthening.

References

1. D. Stöckel, *Min. Invas. Ther. & Allied Technol.,* 9 (2000), pp. 81–88.
2. T.G. Frank, W. Xu, and A. Cuschieri, *Proceedings of the International Conference on Shape Memory and Superelastic Technologies,* ed. S.M. Russell and A.R. Pelton (Pacific Grove, CA: International Organization on SMST, 2001), pp. 549–560.
3. T. Duerig and M. Wholey, *Min. Invas. Ther. & Allied Technol.,* 11 (2002), pp. 173–178.
4. D. Stöckel, C. Bonsignore, and S. Duda, *Min. Invas. Ther. & Allied Technol.,* 11 (2002), pp. 137–147.
5. D. Stöckel, A.R. Pelton, and T. Duerig, *Euro Rad.* (to be published 2003).
6. W. Buehler and F.E. Wang, *Ocean Eng.,* 1 (1968), pp. 105–120.
7. T.W. Duerig et al., eds., *Engineering Aspects of Shape Memory Alloys* (London: Butterworth-Heinemann Ltd., 1990).
8. H. Funakubo, ed., *Shape Memory Alloys* (New York: Gordon and Breach Science Publishers, 1987).
9. L.Mc. Schetky, "Shape Memory Alloys," *Scientific American,* 241 (5) (1979), pp. 74–82.
10. J. Perkins, ed., *Shape Memory Effects in Alloys* (New York: Plenum Press, 1975).
11. T.W. Duerig and A.R. Pelton, "Ti-Ni Shape Memory Alloys," *Materials Properties Handbook: Titanium Alloys,* ed. R. Boyer, G. Welsch, and E.W. Collings (Materials Park, OH: ASM International, 1994), pp. 1035–1048.
12. *ASTM F 2004-00 Test Method for Transformation Temperature of Nickel-Titanium Alloys by Thermal Analysis* (West Conshohocken, PA: ASTM, 2002).
13. C.M. Jackson, H.J. Wagner, and R.J. Wasilewski, *NASA–SP 5110* (Washington, D.C.: DoE Technology Utilization Office, 1972).
14. *ASTM F 2063-00 Standard Specification for Wrought Nickel-Titanium Shape Memory Alloys for Medical Devices and Surgical Implants* (West Conshohocken, PA: ASTM, 2002).
15. S.M. Russell and D.E. Hodgson, *Min. Invas. Ther. & Allied Technol.,* 9 (2000), pp. 61-65.
16. S.M. Russell, *Proceedings of the International Conference on Shape Memory and Superelastic Technologies,* ed. S.M. Russell and A.R. Pelton (Pacific Grove, CA: International Organization on SMST, 2001), pp. 1–10.
17. A.R. Pelton, J. DiCello, and S. Miyazaki, *Min. Invas. Ther. & Allied Technol.,* 9 (2000), pp. 107–118.
18. A.R. Pelton, J. DiCello, and S. Miyazaki, *Proceedings of the International Conference on Shape Memory and Superelastic Technologies,* ed. S.M. Russell and A.R. Pelton (Pacific Grove, CA: International Organization on SMST, 2001), pp. 361–374.
19. T.W. Duerig and R. Zadno, *Engineering Aspects of Shape Memory Alloys,* ed. T.W. Duerig et al. (London: Butterworth-Heinemann Ltd., 1990), pp. 369–393.
20. S. Miyazaki, *Engineering Aspects of Shape Memory Alloys,* ed. T.W. Duerig et al. (London: Butterworth-Heinemann Ltd., 1990), pp. 394–413.
21. M. Nishida, C.M. Wayman, and T. Honma, *Met. Trans. A,* 17A (1986), pp. 1505–1515.

Alan R. Pelton, Scott M. Russell, and John DiCello are with Nitinol Devices & Components in Fremont, California.

For more information, contact A.R. Pelton, Nitinol Devices & Components, a Johnson & Johnson Company, 47533 Westinghouse Drive, Fremont, California 94539 USA; (510) 623-6996; fax (510) 623-6808; e-mail apelton@ndcus.jnj.com.